Multiple Constrained MPC Design For Automotive Dry Clutch Engagement

Journal:	*Transactions on Mechatronics*
Manuscript ID:	Draft
Manuscript Type:	Regular paper
Date Submitted by the Author:	n/a
Complete List of Authors:	Pisaturo, Mario; University of Salerno, Department of Industrial Engineering Cirrincione, Maurizio; University of Technology of Belfort-Montbéliard, FClab-IRTES-SET Senatore, Adolfo; University of Salerno, Department of Industrial Engineering
Keywords:	Predictive control, Road vehicles, Mechanical systems
Are any of authors IEEE Member?:	Yes
Are any of authors ASME Member?:	No

Multiple Constrained MPC Design For Automotive Dry Clutch Engagement

Mario Pisaturo, Maurizio Cirrincione, *Senior Member IEEE*, Adolfo Senatore

***Abstract*—In this paper a multiple Model Predictive Controller (MPC) is proposed for controlling the dry clutch start up phase for automotive applications. Based on high order dynamic model of powertrain system, the feedback controllers are designed by using the crankshaft angular speed and the clutch disk angular speed as measured variables. Moreover, the MPC is developed to comply with constrains both on the input and on the output. The aim of the controller is to ensure a comfortable lock-up and to avoid the stall of the engine as well as to reduce the engagement time. Numerical results show the good performance of the MPC with constrains for avoiding critical operating conditions. Comparisons with similar state-of-the-art works are also shown.**

***Index Terms*— Automated manual transmissions, predictive control with constraints, dry clutch transmissibility, high order model.**

I. Introduction

THE ever increasing use of Automated Manual Transmission (AMT) in modern vehicles has led up to a rapid development of control algorithms for automotive dry clutches.

As a matter of fact, in AMTs the gearshifts phases are managed by an actuator driven by the transmission control unit (TCU), whose control scheme is therefore of utmost importance for obtaining high performance characteristics, like reduction of fuel consumption and pollutant emissions, lower gearshift time, decrease of facing wear and increase of comfort. Conversely, a "bad" control scheme could result in a poor engagement with consequent loss of all advantages obtainable with an AMT.

In order to attain these targets on clutch engagement, several models of control strategies for dry clutches in AMTs have been recently proposed in the literature, like e.g., classical control [1], optimal control [2, 3], predictive control [4, 5], decoupling control [6], and robust control [7, 8]. However, effective AMTs controllers are difficult to be designed without having a physical model of the clutch-torque transmissibility characteristic [9].

Unlike [4, 5], this paper aims at investigating the engagement performance of an actuated dry clutch by taking into account a more detailed frictional characteristic ([10, 11]) and experimental maps of the n-D clutch transmission characteristic [12]. The simulations consider a high-order dynamic system for modeling the passenger car driveline, with a constrained predictive control algorithm, frictional

Mario Pisaturo and Adolfo Senatore are with the Department of Industrial Engineering, University of Salerno, 84084 Fisciano, Italy (e-mail: mpisaturo@unisa.it; a.senatore@unisa.it).

Maurizio Cirrincione is with FClab-IRTES-SET, Université de Technologie de Belfort-Montbéliard, 90000 Belfort, France (e-mail: maurizio.cirrincione@utbm.fr).

and clutch transmission maps, and gear shift maneuvers in several vehicle launch conditions. The solution proposed in this paper is based on the design of a multiple controller working in sequence according to the powertrain operating conditions. These controllers are designed to comply with some constraints which allow the comfort to be improved during the engagement process and increase the safety of the system. This analysis could result in important issues for overcoming the well known poor engagement performance exhibited by AMTs, like engine speed spikes and noise, engine stall and uncomfortable gearshifts.

II. DRIVELINE MODEL

This section describes a model for simulating the driveline dynamic behavior and Figure 1 shows the driveline scheme, where the subscripts *e*, *f*, *c*, *g*, *w* indicate engine, flywheel, clutch disc, (primary shaft of) gearbox, and wheels, respectively. A dynamic model of the driveline can be obtained by applying the torque equilibrium at the different nodes of the driveline scheme, where T indicates the torques, J the inertias and ϑ the angles.

[Fig. 1]

The equations which model the driveline are:

$$J_e\dot{\omega}_e = T_e(\omega_e) - b_e\omega_e - T_{ef}(\vartheta_{ef}, \omega_{ef}) \quad (1)$$

$$J_f\dot{\omega}_f = T_{ef}(\vartheta_{ef}, \omega_{ef}) - T_{fc}(x_{to}) \quad (2)$$

$$J_c\dot{\omega}_c = T_{fc}(x_{to}) - T_{cg}(\vartheta_{cg}, \omega_{cg}) \quad (3)$$

$$J_g(r)\dot{\omega}_g = T_{cg}(\vartheta_{cg}, \omega_{cg}) - b_g\omega_g - 1/r\, T_{gw}(\vartheta_{gw}, \omega_{gw}) \quad (4)$$

$$J_w\dot{\omega}_w = T_{gw}(\vartheta_{gw}, \omega_{gw}) - T_w(\omega_w) \quad (5)$$

and the angle dynamics are:

$$\dot{\vartheta}_e = \omega_e \quad (6)$$

$$\dot{\vartheta}_{ef} = \omega_{ef} = \omega_e - \omega_f \quad (7)$$

$$\dot{\vartheta}_{cg} = \omega_{cg} = \omega_c - \omega_g \quad (8)$$

$$\dot{\vartheta}_{gw} = \omega_{gw} = \omega_g - \omega_w \quad (9)$$

where T_e is the engine torque (assumed to be a control input of the model), $T_{fc}(x_{to})$ is the torque transmitted by the clutch (the second control input), x_{to} is the throwout bearing position, and T_w is the equivalent load torque at the wheels (a measured disturbance). The gear ratio is r (which here includes also the final conversion ratio), and J_c is an equivalent inertia, which includes the masses of the clutch disc, friction pads and the cushion spring.

Furthermore the following equations also hold:

$$J_g(r) = J_{g1} + J_{g2}/r^2 \quad (10)$$

$$T_{ef}(\vartheta_{ef}, \omega_{ef}) = k_{ef}\vartheta_{ef} + b_{ef}\omega_{ef} \quad (11)$$

$$T_{cg}(\vartheta_{cg}, \omega_{cg}) = k_{cg}\vartheta_{cg} + b_{cg}\omega_{cg} \quad (12)$$

$$T_{gw}(\vartheta_{gw}, \omega_{gw}) = k_{gw}\vartheta_{gw} + b_{gw}\omega_{gw} \quad (13)$$

$$T_w(\omega_w) = T_{w0} + \rho_a A c_d R_w^3 \omega_w^2 / 2 \quad (14)$$

where k are torsional stiffness coefficients, b viscous dampings, T_{w0} a constant load torque, ρ_a the air density, A the front surface vehicle area, c_d the air resistance coefficient, R_w the wheels radius.

These equations represent the driveline system during the slipping phase, whereas, during the engaged phase, the flywheel angular speed ω_f and the clutch angular speed ω_c are the same: thus (2) and (3) can be summed each other, which yields:

$$(J_c + J_f)\dot{\omega}_c = T_{ef}(\vartheta_{ef}, \omega_{ef}) - T_{cg}(\vartheta_{cg}, \omega_{cg}) \quad (15)$$

In the continuous state-space representation the driveline model can be written as follows:

$$\begin{aligned} \dot{\mathbf{x}}(t) &= \left[\mathbf{A}_{sl} d + \mathbf{A}_{eng}(1-d)\right]\mathbf{x}(t) \\ &\quad + \left[\mathbf{B}_{sl} d + \mathbf{B}_{eng}(1-d)\right]\mathbf{u}(t) \\ \mathbf{y}(t) &= \mathbf{C}\mathbf{x}(t) \end{aligned} \quad (16)$$

where the state, input and output vectors are respectively:

$$\mathbf{x} = \{\omega_e \quad \vartheta_e \quad \omega_f \quad \vartheta_f \quad \omega_c \quad \vartheta_c \quad \omega_g \quad \vartheta_g \quad \omega_w \quad \vartheta_w\}^T$$

$$\mathbf{u} = \{T_e \quad T_{fc} \quad T_w\}^T$$

$$\mathbf{y} = \{\omega_e \quad \omega_c\}^T$$

and d is a switching variable equal to 1 when the system is in the slipping phase and 0 otherwise. The subscript *'sl'* and *'eng'* indicate the slipping and the engaged system matrices, respectively, and the matrices can be simply deduced from (1)-(15).

III. CONSTRAINTS

Some constraints have been considered to design the MPC in order to avoid the engine stall condition and to guarantee a comfortable lock-up.

A. Constraints on the "plant" input

Saturation constraints have been imposed both on the torques and on their variation rates:

$$T_e \in \left[T_e^{\min}, T_e^{\max}\right] \quad (17)$$

$$T_{fc} \in \left[T_{fc}^{\min}, T_{fc}^{\max}\right] \quad (18)$$

$$\dot{T}_e \in \left[\dot{T}_e^{\min}, \dot{T}_e^{\max}\right] \quad (19)$$

where $T_e^{\min} = 0$ Nm is the minimum engine torque value during the vehicle launch, $T_e^{\max} = 250$ Nm is the maximum engine torque value, $T_{fc}^{\min} = 0$ Nm is the minimum torque value transmitted by the clutch, $T_{fc}^{\max} = 315$ Nm is the maximum torque value that the clutch can transmit, $\dot{T}_e^{\min} = -500$ Nm/s is the maximum decrease (≤ 0) in one step

and $\dot{T}_e^{\max} = 500$ Nm/s is the maximum increase (≥ 0) in one step.

B. Constraints on the "plant" output

On the engine and clutch angular speeds, the following constraints hold:

$$\omega_e \in \left[\omega_e^{kill}, \omega_e^{\max} \right] \tag{20}$$

$$\omega_c \geq \omega_c^{\min} \tag{21}$$

where $\omega_e^{kill} = 80$ rad/s represents the so-called no-kill condition [6], $\omega_e^{\max} = 600$ rad/s is the maximum value of the engine speed before attaining critical conditions and $\omega_c^{\min} = 0$ rad/s is the minimum value of clutch speed during the vehicle launch. It is worth noting that it is not necessary to impose a maximum clutch angular speed, because it is equal to the engine angular speed during the engaged phase and it can only decrease for passive resistance during the idle phase.

IV. MPC DESIGN

As explained above, the driveline can have two different working conditions: the slipping phase and the engaged phase. That is why two different controllers for each phase have been designed. The switching parameter *d* selects the controller by considering the absolute value of the difference between the engine and the clutch angular speed. Particularly, the switching condition is attained when $\omega_{sl} = |\omega_e - \omega_c| \leq 1$ rad/s. It is important to emphasize that in no way the two controllers can work simultaneously and so any conflict between them is avoided prior.

The MPC has been designed with the discrete time version of the driveline model (16) obtained by using the zero-order hold method with a sampling time of 0.01 s.

$$\begin{aligned} \mathbf{x}_{k+1} &= \left[\bar{\mathbf{A}}_{sl} d + \bar{\mathbf{A}}_{eng} (1-d) \right] \mathbf{x}_k + \left[\bar{\mathbf{B}}_{sl} d + \bar{\mathbf{B}}_{eng} (1-d) \right] \mathbf{u}_k \\ \mathbf{y}_k &= \bar{\mathbf{C}} \mathbf{x}_k \end{aligned} \tag{22}$$

The MPC aims a finding the output $\mathbf{y}_k$ by tracking the reference trajectory $\mathbf{r}_k$ and fulfilling the constraints seen above for any time step $k \geq 0$.

Under the assumption that the estimate of $\mathbf{x}_k$ is available at time k, the cost function to be optimized is:

$$\begin{aligned} J_i(\Delta u, \varepsilon) &= \mathbf{u}_i{}^T \mathbf{W}_{u,i}^2 \mathbf{u}_i + \Delta \mathbf{u}_i{}^T \mathbf{W}_{\Delta u,i}^2 \Delta \mathbf{u}_i + \ldots \\ &+ \left[\mathbf{y}_i - \mathbf{r}_i \right]^T \mathbf{W}_{y,i}^2 \left[\mathbf{y}_i - \mathbf{r}_i \right] + \rho_\varepsilon \varepsilon \end{aligned} \tag{23}$$

where $\mathbf{u}_i = \left[u_i(0) \ \ldots \ u_i(p-1) \right]^T$ is the input vector, $\Delta \mathbf{u}_i = \left[\Delta u_i(0) \ \ldots \ \Delta u_i(p-1) \right]^T$ is the input increment vector, $\mathbf{y}_i = \left[y_i(0) \ \ldots \ y_i(p) \right]^T$ is the output vector; $\mathbf{r}_i = \left[r_i(0) \ \ldots \ r_i(p) \right]^T$ is the reference trajectory vector, $\mathbf{W}_{u,i}$,

$\mathbf{W}_{\Delta u,i}$ and $\mathbf{W}_{y,i}$ are, respectively, the input, input increment and output weights matrices (diagonals and squares); finally, the subscript $i = 1,2$ accounts for the two inputs and two outputs of the "plant". The constraints on $\mathbf{u}$, $\Delta\mathbf{u}$, and $\mathbf{y}$ are softened by introducing the slack variable $\varepsilon \geq 0$. In (23), the weight ρ_ε on the slack variable ε penalizes the violation of the constraints. As ρ_ε increases with respect to the input and output weights, the controller gives a higher priority to the minimization of constraint violations.

The optimization accounts for the constrains as follows:

$$\begin{cases} u_{\min,i}(j) - \varepsilon V^{u}_{\min,i}(j) \leq u_i(k+j|k) \leq u_{\max,i}(j) \\ \qquad + \varepsilon V^{u}_{\max,i}(j) \\ \Delta u_{\min,i}(j) - \varepsilon V^{\Delta u}_{\min,i}(j) \leq \Delta u_i(k+j|k) \leq \Delta u_{\max,i}(j) \\ \qquad + \varepsilon V^{\Delta u}_{\max,i}(j) \\ y_{\min,i}(j) - \varepsilon V^{y}_{\min,i}(j) \leq y_i(k+j+1|k) \leq y_{\max,i}(j) \\ \qquad + \varepsilon V^{y}_{\max,i}(j) \\ \Delta u_i(k+h|k) = 0 \\ \varepsilon \geq 0 \end{cases} \tag{24}$$

where $j = 0,...,P-1$, $h = m,...,P-1$, P is the prediction horizon, m is the control horizon, the vectors $V^{u}_{\min,i}$, $V^{u}_{\max,i}$, $V^{\Delta u}_{\min,i}$, $V^{\Delta u}_{\max,i}$, $V^{y}_{\min,i}$, $V^{y}_{\max,i}$ have nonnegative entries that quantify the concern for relaxing the corresponding constraint; the larger V, the softer the constraint. $V = 0$ means that the constraint is hard and cannot be violated. The following constraints have been considered hard for the input and input increments: $V^{u}_{\min,i} = V^{u}_{\max,i} = V^{\Delta u}_{\min,i} = V^{\Delta u}_{\max,i} = 0$, whereas the soft constraints for the outputs are $V^{y}_{\min,i} = V^{y}_{\max,i} = 1$

A. Tuning

The parameters to be tuned are the prediction horizon P, the control horizon m, the weights W_u, $W_{\Delta u}$, W_y, respectively, the input, the input increments, the output weights matrices, and the overall penalty weight ρ_ε. In the first phase the parameters are tuned in simulation until the desired performance is achieved by using Simulink® and the MPC Toolbox. The trade-off between fast engagement and comfortable lock-up is easily achievable by suitably choosing the weights W_u, $W_{\Delta u}$ and W_y. Instead, the prediction and the control horizon, together with the input weight, allow the steady-state solution to be improved. The parameters used during the simulations are defined in the next paragraphs.

B. MPC1 parameters - slipping phase

Table 1 shows the parameters used for the MPC during the slipping phase:

[Table 1]

C. MPC2 parameters - engaged phase

Table 2 shows the parameters used for the MPC during the engaged phase:

[Table 2]

D. Closed-loop control scheme

This section analyses the AMT closed loop control scheme. The driveline model parameters are shown in Table 3. The simulations are carried out by using a closed loop system with two MPCs as described in the previous paragraph for the slipping and engaged phases. The set point inputs are the $\omega_{e,sp}$ and the $\omega_{c,sp}$ (see Fig. 2 for details). The set point about clutch angular speed $\omega_{c,sp}$ and engine speed $\omega_{e,sp}$ are compared with the output of the driveline model. The parameters of the MPC are shown in Tables 1 and 2, respectively. The first output of the MPC, the engine torque T_e is fed directly into the driveline model. Instead, the second output of the MPC, the clutch torque T_{fc}, is inverted by using the cushion spring load-deflection characteristic and the friction coefficient μ_0 in order to obtain the reference throwout bearing position x_{to}^{ref}. The latter variable is modified by means of a controlled actuator which is represented by considering the discrete time model of a unitary gain first-order transfer function with a time constant equal to 0.1 s. In the control scheme the actuator transfer function is $A(z)=\dfrac{0.0952}{z-0.905}$. The output of $A(z)$ is the throwout bearing position which is used as an input of the clutch torque map in order to obtain the clutch torque to use in the dynamic model. The clutch torque map is given by (25), [13, 14]:

$$T_{fc}\ (x_{to}) = n\mu(v,p)R_{eq}F_{fc}(\delta_f(x_{pp}(x_{to}))) \qquad (25)$$

where the clutch-torque transmissibility model assumes the torque T_{fc} to be proportional to the cushion spring load-deflection characteristic $F_{fc}(\delta_f)$ through the dynamic friction coefficient $\mu(v,p)$, the number of friction surfaces n and the geometrical parameter R_{eq}. Particularly, the cushion spring load-deflection characteristic $F_{fc}(\delta_f)$ depends on the push plate position x_{pp} and they both depend on the throwout bearing position x_{to}. The latter being the second control variable of the considered AMT system. Instead, the dynamic friction depends on the sliding speed $v = R_{eq}\omega_{sl}$ and the contact pressure p. Fig. 2 shows a detail of an engagement system in the kiss position and explains the physical meanings of the variables introduced above.

[Fig. 2]

In the numerical algorithm, the cushion spring characteristics is a look-up table [10, 12], whereas, the friction coefficient, function of the

contact pressure and of the sliding speed, has been obtained as in [11, 15]. The closed loop control scheme is shown in Figure 3.

[Fig. 3]

V. Simulation Results

This section describes the results of the simulations to show the difference between the constrained and the unconstrained MPC during the vehicle launch. The clutch is considered to be engaged when the value of the slip speed is less than 1 rad s^{-1}. Once the clutch is engaged, the throwout bearing position is rapidly increased to its maximum value by the control algorithm. The subparagraphs below show the results for two different launch maneuvers.

A. Maneuver 1

The figures below show the results of a typical launch maneuver. Fig. 4 shows the plots of the engine (a) and the clutch (b), angular speeds, respectively. The dashed blue lines represent the set points $\omega_{e,sp}$ and $\omega_{c,sp}$, the solid red lines represent the output of the constrained model $\omega_{e,C}$ and $\omega_{c,C}$ whereas the green dash-dot lines represent the output of the unconstrained model $\omega_{e,U}$ and $\omega_{c,U}$. For the clutch speed there are not differences between the outputs of the two models. For the engine speed, instead, there are some little differences as shown in Fig. 4 a.

[Fig. 4]

Fig. 5 shows the MPC outputs $T_e\,MPC$ $T_{fc}\,MPC$, the torque load T_{load} and the clutch torque output of the clutch model map block T_{fc}.

[Fig. 5]

This picture highlights that both MPC outputs do not violate their lower bounds (a). This violation instead occurs in the unconstrained model (b). The green dotted line represents the clutch torque output of the clutch torque map block. After that the engaged condition is attained, the throwout bearing position reaches its maximum value, as shown in Fig. 6, corresponding to the maximum torque transmittable by the clutch by considering the frictional map and the cushion spring characteristics.

[Fig. 6]

Moreover, it is important to note that the unconstrained MPC impose negatives values to the throwout bearing position resulting in a dangerous and unwanted condition, i.e. excessive stress on the actuator that may be damaged. To avoid this a saturator on the actuator output is necessary. On the other hand the constrained controllers never reach negative values making this saturator unnecessary.

[Fig. 7]

Fig. 7 describes the engine and clutch angular speed set point (a), and the outputs of the driveline both for the unconstrained and the constrained model (b). It shows that the engagement time is 2.8 s for

the set points and 1.7 s for the driveline outputs: this results in reduction of wear of frictional facings, less energy and fuel consumptions. Moreover, it is possible to note that the start up manoeuvre with the unconstrained model produces an engine speed spike, with consequent noise, and undesired jerks.

[Fig. 8]

Finally, Fig. 8 shows the input/output trajectories both for the constrained model and for the unconstrained model. In this picture it is apparent how the constrained MPC keeps both the input and the output within the limits, represented by the black parallelepipeds.

B. Maneuver 2

This section presents the results of a fast launch manoeuvre. Fig. 9 shows the engine (a) and the clutch (b) angular speeds, respectively. Also in this case there are no differences for the clutch speed between the two models. However there is a remarkable difference between the engine speed of the constrained and unconstrained model (Fig. 8 a). This is due to the fast torque demanded for this maneuver as highlighted also in Fig. 9. Actually, in this figure, by comparing the image (a) with the image (b), it is possible to note how the constraints, both on the engine torque and on its rate, play an important role to prevent the violation of the limits (red solid lines). In the same figure it is possible to note that the clutch torque in both cases is nearly the same (blue dashed lines).

[Fig. 9]

[Fig. 10]

In this case the unconstrained MPC imposes high negatives values to the throwout bearing, which compromises the system security. Fig. 10 a shows that the constrained controllers, also for a fast torque demand, never reach negatives values of x_{to}.

[Fig. 11]

Also Fig. 12 shows that the engagement time is 2.4 s for the set points and 1.9 s for the driveline outputs. Moreover, it is noteworthy the start-up maneuver with the unconstrained controllers produces an engine speed spike, with resulting noise, and undesired jerks.

[Fig. 12]

Finally, Fig. 13 highlights the good performance of the constrained MPC preventing the limits to be exceeded.

[Fig. 13]

C. Optimized MPCs for a reduced order model of the driveline

This section shows the simulations results of the constrained MPCs tuned for a reduced order driveline [4, 5], but used to control the high order driveline described in this paper, which better represents the real system. As explained in [4, 5] the reduced order model of the driveline can be controlled by using only one MPC. However the simulations

carried out show that it is impossible to control a real system by using only one controller.

Actually, Fig. 14, 15, 16 and 17 illustrate that, after that the engagement condition is reached, the controller cannot manage the lock-up phase at the same time.

[Fig. 14]

[Fig. 15]

[Fig. 16]

[Fig. 17]

Thus, a second controller is necessary to overcome this problem.

As shown below, by introducing an optimized second controller also on the reduced order model, it is possible to control a high order model.

Table 3 shows the parameters used for the MPC optimized for a reduced order model during the slipping phase:

[Table 3]

Table 4 shows the parameters used for the MPC optimized for a reduced order model during the engaged phase:

[Table 4]

D. Maneuver 1

The Fig. 18 shows the comparison between the engine angular speed, set point and output, a), and the clutch angular speed set point and output, b).

[Fig. 18]

It is noteworthy the start-up maneuver with the constrained controllers optimized for a reduced order model produces a slight increase of the jerks, Fig. 18 and 19.

[Fig. 19]

Finally, Fig. 20 shows the torque values as a function of the time.

[Fig. 20]

E. Maneuver 2

Fig. 21 shows the comparison between the engine angular speed, set point and output, a), and the clutch angular speed set point and output, b).

Also in this case it is possible to note that the start-up maneuver with the constrained controllers optimized for a reduced order model produces a slight increase of the jerks, Fig. 21 and 22.

[Fig. 21]

[Fig. 22]

Finally, Fig. 23 shows the torque values as a function of the time. This graph, together with Fig. 20, shows how the controllers impose sudden changes of the engine torque during the launch maneuver, which results in increase of the jerks.

[Fig. 23]

VI. Conclusions

A multiple model predictive controller for dry clutch engagement problem during vehicle launch has been proposed. Two controllers, the first for the slipping phase and the second for the engaged phase, have been designed to get a good trade-off between a fast engagement and a comfortable maneuver by complying with the imposed limits both on the input and the output variables.

Simulation results have shown that a good choice of the MPC parameters and the adoption of constrained controllers make it possible to achieve better performance in terms of safety of the system and comfortable engagement process.

A comparison with a similar work in literature is also presented, showing the necessity of 2 MP controllers.

As future work the MPC will be used to test its behavior during different working conditions like upshift and downshift maneuvers. Finally, the possibility to implement this algorithm on real-time system will be considered.

Appendix

The driveline parameter values are listed below [1, 5].

[Appendix]

References

[1] G. Lucente, M. Montanari e C. Rossi, “Modelling of an Automated Manual Transmission System, ” Mechatronics, vol. 17, pp. 73-91, 2007.
[2] L. Glielmo e F. Vasca, “Optimal Control of Dry Clutch Engagement,” in SAE 2000 World Congr., Detroit, MI, 2000.
[3] P. Dolcini, C. Canudas de Wit e H. Bechart, “Lurch Avoidance Strategy and its Implementation in AMT Vehicles,” Mechatronics, vol. 18, pp. 289-300, 2008.
[4] A. Bemporad, F. Borrelli, L. Glielmo e F. Vasca, “Hybrid Control of Dry Clutch Engagement,” in Eur. Control Conf., Porto, Portugal, 2001.
[5] R. Amari, M. Alamir e P. Tona, “Unified MPC Strategy for Idle Speed Control, Vehicle Start-up and Gearing Applied to an Automated Manual Transmission,” in 17th IFAC World Congr., Seoul, South Korea, 2008.
[6] L. Glielmo, L. Iannelli, V. Vacca e F. Vasca, “Gearshift control for automated manual transmissions, ” IEEE/ASME Trans. Mechatronics, vol. 11, n. 1, pp. 17-26, February 2006.
[7] L. Glielmo, P. O. Gutman, L. Iannelli e F. Vasca, “Robust Smooth Engagement of an Automotive Dry Clutch,” in Proc. 4th IFAC Symp. Mechatronics Syst., Heidelberg, Germany, 2006.
[8] G. J. L. Naus, M. Beenakkers, R. Huisman, M. J. G. van de Molengraft e M. Steinbuch, “Robust Control to Suppress Clutch Judder,” in 8th Int. Symp. Adv. Veh. Control, Kobe, Japan, 2008.
[9] F. Vasca, L. Iannelli, A. Senatore e G. Reale, “Torque Transmissibility Assessment for Automotive Dry-Clutch Engagement, ” IEEE/ASME Transaction on Mechatronics, vol. 16, n. 3, pp. 564-573, June 2011.

[10] V. D'Agostino, N. Cappetti, M. Pisaturo e A. Senatore, "Improving The Engagement Smoothness Through Multi-Variable Frictional Map In Automated Dry Clutch Control," in ASME2012 International Mechanical Engineering Congress & Exposition, Houston, Texsas, 2012.
[11] V. D'Agostino, A. Senatore e M. Pisaturo, "Improving the engagement performance of automated dry clutch through the analysis of the influence of the main parameters on the frictional map," in World Tribology Congress 2013, Torino, Italy, 2013, accepted.
[12] N. Cappetti, M. Pisaturo e A. Senatore, "Modelling the Cushion Spring Characteristic to Enhance the Automated Dry-Clutch Performance: the Temperature Effect," Proc IMech Part D: J Autom Eng, vol. 226, n. 11, pp. 1472-1482, 2012.
[13] F. Vasca, L. Iannelli, A. Senatore e M. Taglialatela Scafati, "Modeling Torque Transmissibility for Automotive Dry Clutch Engagement," in American Control Conference 2008, 2008.
[14] N. Cappetti, M. Pisaturo e A. Senatore, "Cushion spring sensitivity to the temperature rise in automotive dry clutch and effects on the frictional torque characteristic," Mechanical Testing and Diagnosis, vol. 3, n. II, pp. 28-38, 2012.
[15] A. Senatore, V. D'Agostino, R. Di Giuda e V. Petrone, "Experimental investigation and neural network prediction of brakes and clutch material frictional behaviour considering the sliding acceleration influence," Tribology International,, vol. 44, pp. 1199-1207, 2011.

Mario Pisaturo was born in 1984 in Salerno, Italy. He received his Second Level Degree in Mechanical Engineering with honors in 2010 at the University of Salerno. In the same year he obtained the qualification to engineering profession.

He is currently pursuing the Ph.D. degree in mechanical engineering at the Department of Industrial Engineering (DIIN) of the University of Salerno.

The main research topic is: analysis theoretical/experimental of dry clutches for automotive with regard to automated manual transmissions. He takes part in the subject area Applied Mechanics.

Mautizio Cirrincione (M'03) received the "Laurea" degree from the Politecnico di Torino, Turin, Italy, in 1991, and the Ph.D. degree from the University of Palermo, Palermo, Italy, in 1996, both in electrical engineering. From 1996 to 2005 he was a Researcher with the I.S.S.I.A.-C.N.R. Section of Palermo (Institute on Intelligent Systems for Automation), Palermo, Italy. Since 2005 he is Full Professor of Control Systems at the UTBM (University of Technology of Belfort-Montbéliard) in France and member of the IRTES-Set Laboratory.

His current research interests are neural networks for modeling and control, system identification, intelligent control, power electronics, power quality, renewable energy systems, control of fuel cell systems, hybrid vehicles, and electrical machines and drives with rotating or linear AC motors.

Dr. Cirrincione was awarded the 1997 "E.R.Caianiello" prize in 1997 for the best Italian Ph.D. thesis on neural networks. He is author of over 130 papers, 50 of which on high impact factor journals, and of two books.

Adolfo Senatore received the M.Sc. degree in Mechanical Engineering in 1998 from the University of Salerno and the Ph.D. degree in Tribology from University of Pisa in 2002.

He has been Researcher of Mechanics for Machine Systems with the Department of

Industrial Engineering - University of Salerno, while he has been serving as teacher of Mechanical Measurements and Mechatronics since 2004. His scientific work is documented by more than 110 scientific papers in the following areas: frictional modelling in automotive transmissions, lubrication in internal combustion engines and journal bearings, effects of nanoparticles as friction reducer additives, vibration measurement methods. During 2012, he visited as guest professor the Department of Applied Mechanics of the Technische Universität Berlin with a grant from DAAD. He served as reviewer for several journals on the topics of Mechanics, Mechatronics, Tribology.

Dr. Senatore is Member of Nano_Mates, research centre for nanomaterials and nanotechnology of the same Institution.

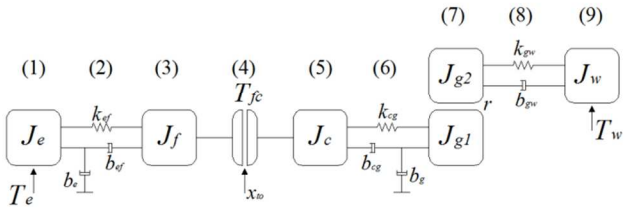

Fig. 1 Driveline scheme.

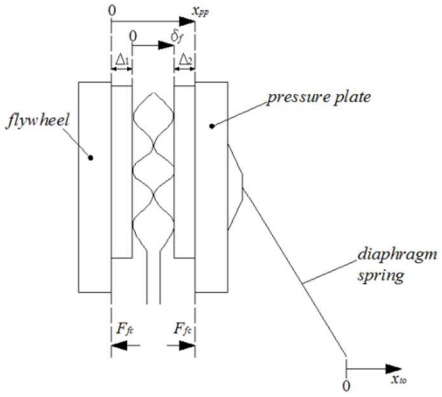

Fig. 2 Clutch system in the kiss point position.

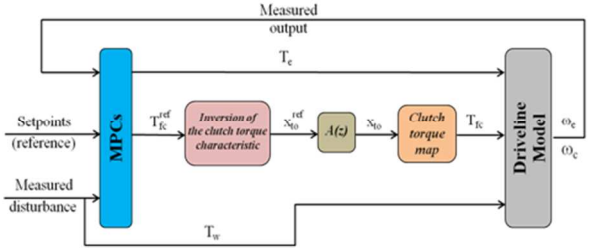

Fig. 3 Closed loop control scheme.

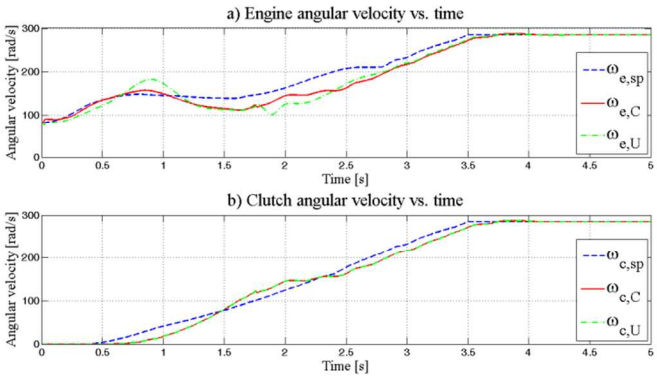

Fig. 4 Engine a) and Clutch b) angular speed.

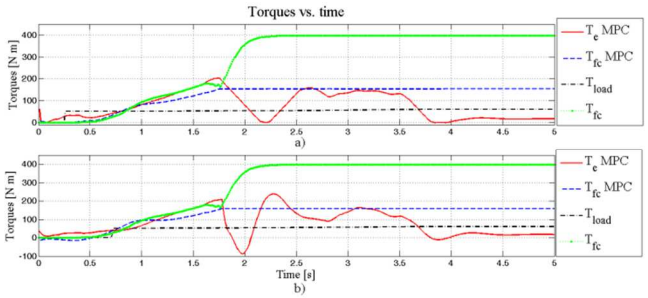

Fig. 5 Torques a) Constrained and b) Unconstrained.

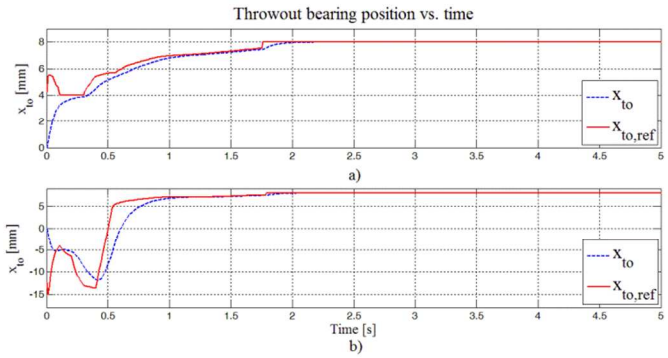

Fig. 6 Throwout bearing position a) Constrained and b) Unconstrained.

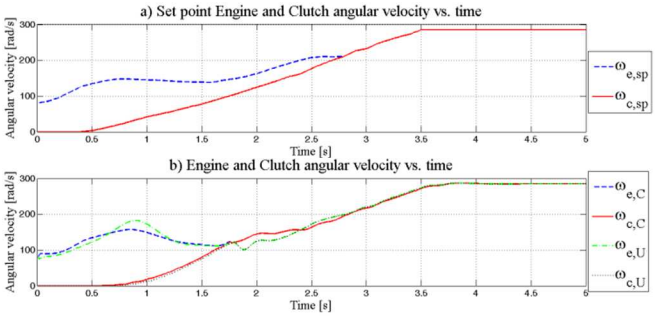

Fig. 7 Engine and clutch speed a) Set points b) Driveline outputs.

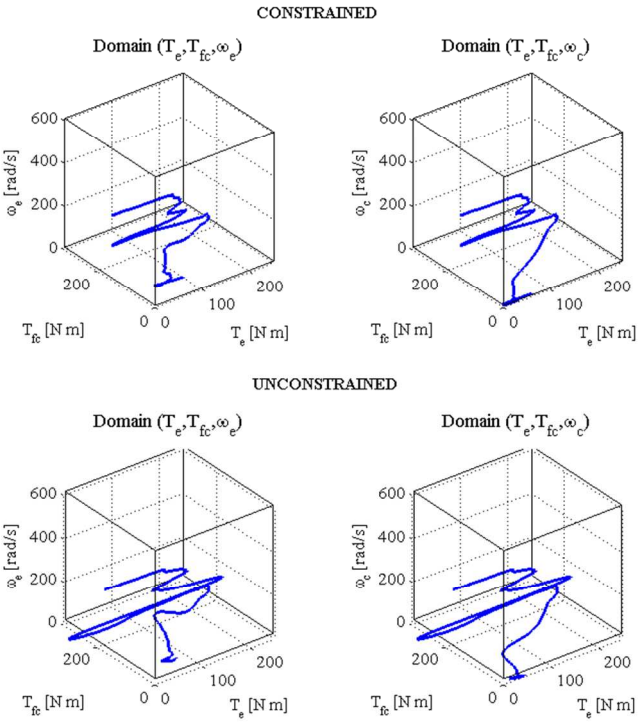

Fig. 8 Input/Output trajectories.

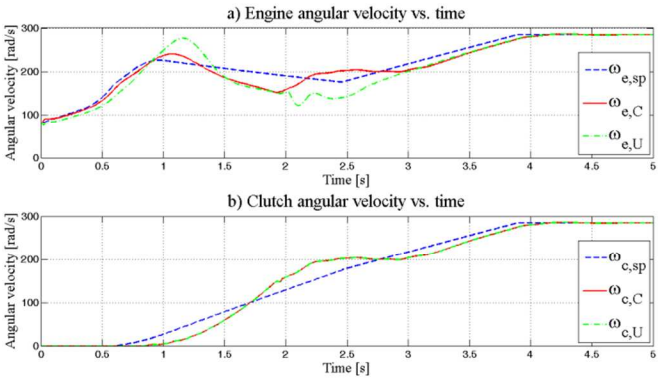

Fig. 9 Engine a) and Clutch b) angular speed.

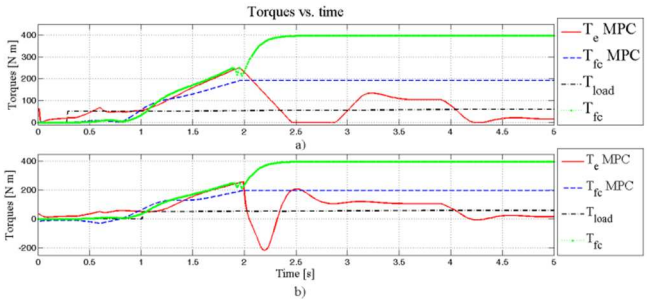

Fig. 10 Torques a) Constrained and b) Unconstrained.

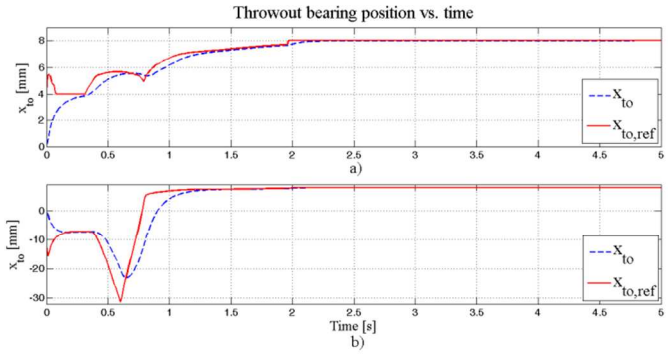

Fig. 11 Throwout bearing position a) Constrained and b) Unconstrained.

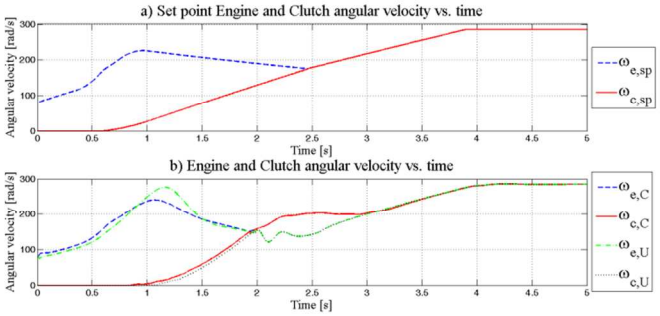

Fig. 12 Engine and clutch speed a) Set points b) Driveline outputs.

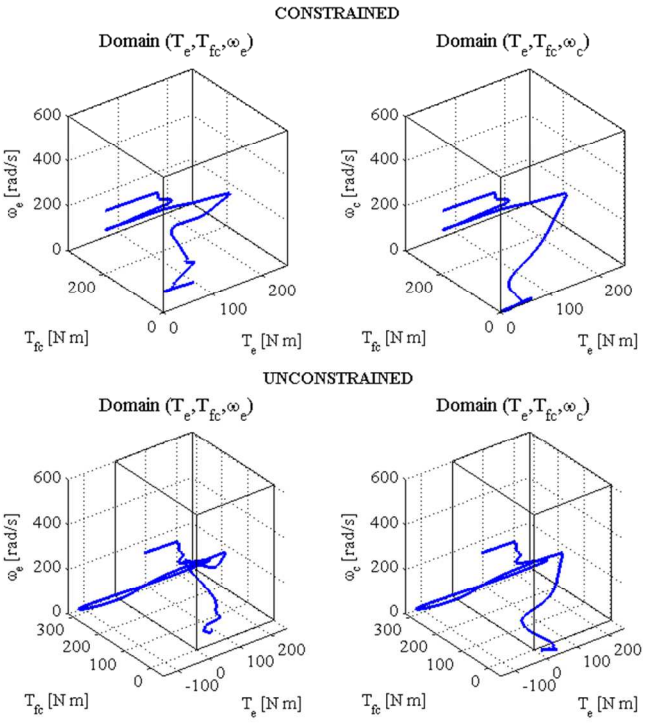

Fig. 13 Input/Output trajectories.

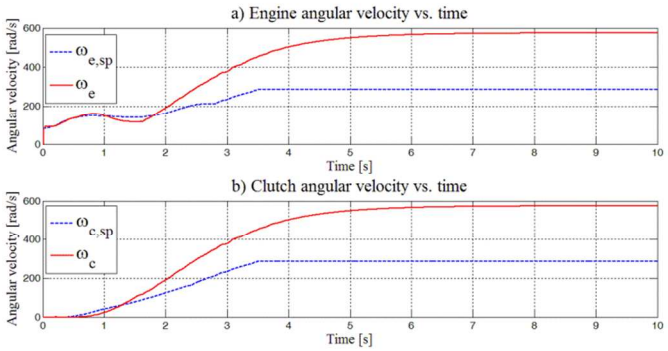

Fig. 14 Maneuver 1: Engine a) and Clutch b) angular speed.

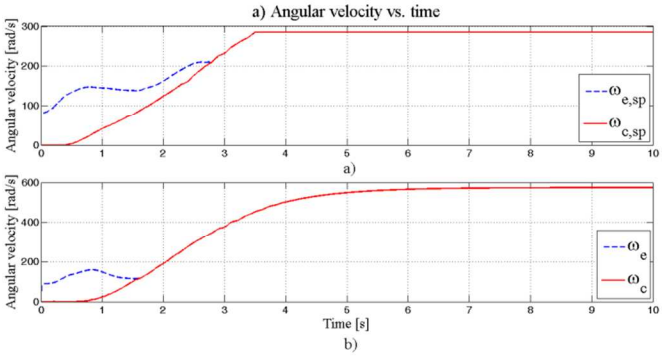

Fig. 15 Maneuver 1: Engine and clutch speed a) Set points b) Driveline outputs.

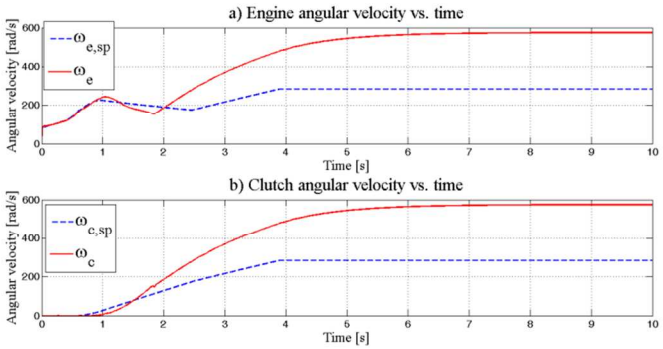

Fig. 16 Maneuver 2: Engine a) and Clutch b) angular speed.

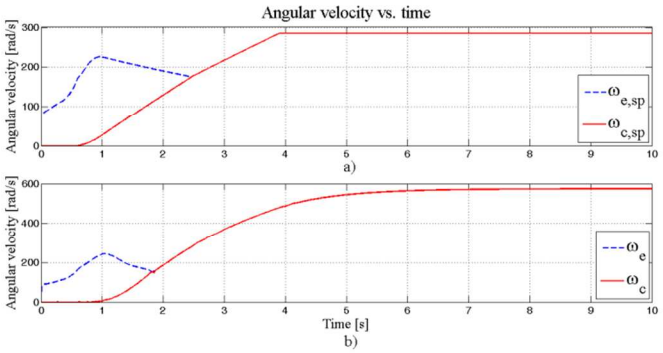

Fig. 17 Maneuver 2: Engine and clutch speed a) Set points b) Driveline outputs.

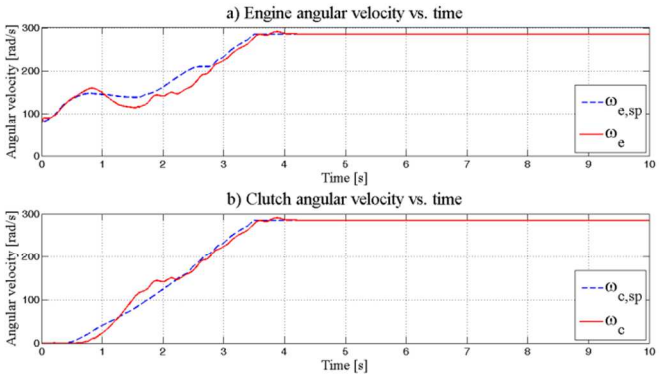

Fig. 18 Engine a) and Clutch b) angular speed.

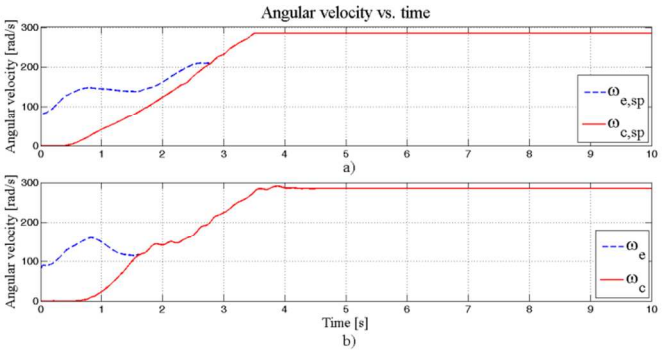

Fig. 19 Engine and clutch speed a) Set points b) Driveline outputs.

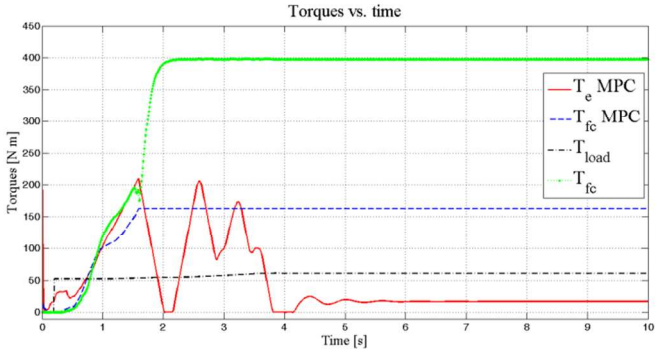

Fig. 20 Torques vs. time.

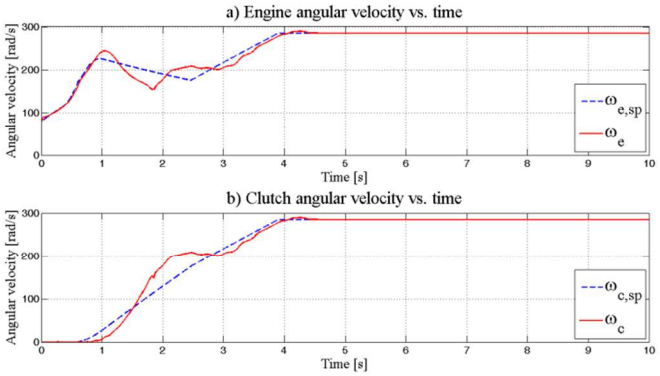

Fig. 21 Engine a) and Clutch b) angular speed.

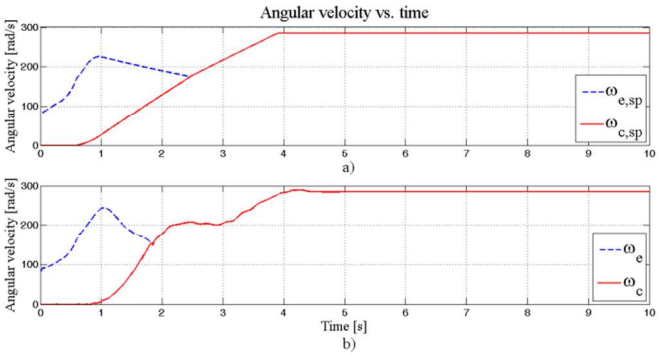

Fig. 22 Engine and clutch speed a) Set points b) Driveline outputs.

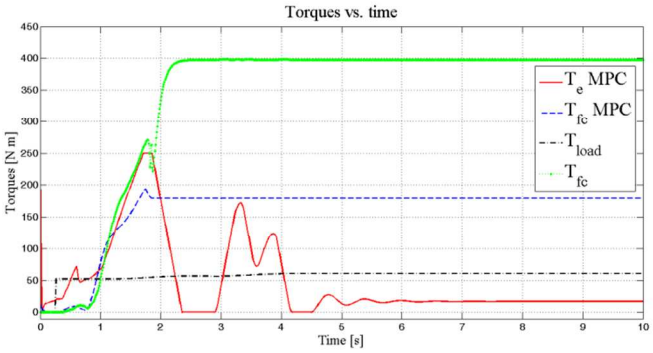

Fig. 23 Torques vs. time.

TABLE I
MPC1 PARAMETERS, SLIPPING PHASE

Symbol	Description	Value	
		1	2
W_u	Input weight	0.18	0.12
$W_{\Delta u}$	Input rate weight	0.15	0.35
W_y	Output weight	1.00	1.15
P	Prediction horizon	10	
m	Control horizon	2	
ρ_ε	Overall penalty weight	0.8	

TABLE II
MPC2 PARAMETERS, ENGAGED PHASE

Symbol	Description	Value	
		1	2
W_u	Input weight	0	0
$W_{\Delta u}$	Input rate weight	1	0
W_y	Output weight	1	1
P	Prediction horizon	15	
m	Control horizon	5	
ρ_ε	Overall penalty weight	0.8	

TABLE III
MPC1 - 2 DoF PARAMETERS, SLIPPING PHASE

Symbol	Description	Value	
		1	2
W_u	Input weight	0.1	0.1
$W_{\Delta u}$	Input rate weight	0.1	0.1
W_y	Output weight	1	1
P	Prediction horizon	10	
m	Control horizon	2	
ρ_ε	Overall penalty weight	0.8	

TABLE IV
MPC2 - 2 DoF PARAMETERS, ENGAGED PHASE

Symbol	Description	Value	
		1	2
W_u	Input weight	0	0
$W_{\Delta u}$	Input rate weight	1	0
W_y	Output weight	1	1
P	Prediction horizon	15	
m	Control horizon	5	
ρ_ε	Overall penalty weight	0.8	

APPENDIX

Symbol	Description	Value
ρ_a	Air density	1.2 kg m^{-3}
Δ	$\mu_d - \mu_s$	-
$\dot{\omega}_c$	Clutch angular acceleration	rad s^{-2}
ω_c	Clutch angular speed	rad s^{-1}
ω_e^{sp}	Set point engine angular speed	rad s^{-1}
ω_c^{sp}	Set point clutch angular speed	rad s^{-1}
$\dot{\omega}_e$	Engine angular acceleration	rad s^{-2}
ω_e, $\dot{\vartheta}_e$	Engine angular speed	rad s^{-1}
$\dot{\omega}_f$	Flywheel angular acceleration	rad s^{-2}
ω_{ef}, $\dot{\vartheta}_{ef}$	Crankshaft angular speed	rad s^{-1}
ϑ_{ef}	Crankshaft angle	rad
$\dot{\omega}_g$	Main shaft angular acceleration	rad s^{-2}
ω_g, ω_{cg}, $\dot{\vartheta}_{cg}$	Main shaft angular speed	rad s^{-1}
ϑ_{cg}	Main shaft angle	rad
$\dot{\omega}_w$	Wheel angular acceleration	rad s^{-2}
ω_{gw}, $\dot{\vartheta}_{gw}$	Driveshaft angular speed	rad s^{-1}
ϑ_{gw}	Driveshaft angle	rad
δ_f	Cushion spring compression	mm
μ_s, μ_d	Static (dynamic) friction coefficient	-
A	Front surface vehicle area	2.12 m^2
c_d	Air resistance coefficient	0.367
F_{fc}	Reaction of the cushion spring	N
J_c	Equivalent clutch disc inertia	0.0159 kg m^2
J_e	Equivalent engine inertia	0.159 kg m^2
J_f	Equivalent flywheel inertia	0.0159 kg m^2
J_g	$J_{g1} + \frac{J_{g2}}{r^2}$	0.0393 kg m^2
J_{g1}	Equivalent gearbox primary shaft	0.039 kg m^2
J_{g2}	Equivalent gearbox secondary shaft	0.039 kg m^2
J_v	Equivalent vehicle inertia at main shaft	0.942 kg m^2
J_w	Equivalent wheel inertia	133 kg m^2
n	Number of friction surfaces on the clutch disc	2
R_{eq}	Equivalent radius of the contact surface	0.089 m
R_w	Wheel radius	0.32 m
t	Time	s
T_{cg}	Main shaft torque	N m
T_e^{ref}, T_e	Engine torque	N m
T_{ef}	Engine-flywheel torque	N m

T_{fc}	Torque transmitted by clutch	N m
T_{fc}^{ref}	Reference torque transmitted by clutch	N m
T_{gw}	Driveshaft torque	N m
T_{w}	Equivalent torque load at wheel	N m
T_{w0}	Load torque	52 N m
v	Sliding speed	m s^{-1}
b_{e}	Engine friction coefficient	0.03 kg m^2 s^{-1}
b_{g}	Main shaft friction coefficient	0.012 kg m^2 s^{-1}
b_{ef}	Crankshaft viscous damping	100 kg m^2 s^{-1}
b_{cg}	Main shaft viscous damping	4 kg m^2 s^{-1}
k_{ef}	Crankshaft torsional stiffness coefficient	32 10^3 kg m^2 s^{-2}
k_{cg}	Main shaft torsional stiffness coefficient	3.2 10^3 kg m^2 s^{-2}
k_{gw}	Driveshaft torsional stiffness coefficient	16 10^3 kg m^2 s^{-2}
r	Gear ratio (included the final conversion ratio)	12.135
x_{pp}	Pressure plate position	mm
x_{to}	Throwout bearing position	mm
x_{to}^{ref}	Reference throwout bearing position	mm
x_{to}^{cnt}	Throwout bearing position at kiss point	mm
x_{to}^{cls}	Throwout bearing position at clutch closed	mm
$x_{to}^{\max}$	Throwout bearing maximum position	mm